AFRL-RV-PS-
TR-2023-0074

AFRL-RV-PS-
TR-2023-0074

TRACKING GNSS-LIKE SIGNALS TRANSMITTED FROM LEO SATELLITES AND PROPAGATED THROUGH IONOSPHERIC PLASMA IRREGULARITIES

Jiawei Xu, et al.

University of Colorado Boulder
552 UCB
Boulder, CO 80309-0552.

03 June 2023

Final Report

APPROVED FOR PUBLIC RELEASE; DISTRIBUTION IS UNLIMITED.

AIR FORCE RESEARCH LABORATORY
Space Vehicles Directorate
3550 Aberdeen Ave SE
AIR FORCE MATERIEL COMMAND
KIRTLAND AIR FORCE BASE, NM 87117-5776

DTIC COPY

NOTICE AND SIGNATURE PAGE

AFRL-RV-PS-TR-2023-0074 HAS BEEN REVIEWED AND IS APPROVED FOR PUBLICATION IN ACCORDANCE WITH ASSIGNED DISTRIBUTION STATEMENT.

//SIGNED//

Dr. Joanna C. Hinks
Program Manager, AFRL/RVB

//SIGNED//

Mark E. Roverse, Chief
AFRL Geospace Technologies Division

REPORT DOCUMENTATION PAGE	*Form Approved OMB No. 0704-0188*

1. REPORT DATE *(DD-MM-YYYY)*	**2. REPORT TYPE**	**3. DATES COVERED** *(From - To)*
03-06-2023	Final Report	03 Sep 2019 – 03 May 2023

4. TITLE AND SUBTITLE
Tracking GNSS-like Signals Transmitted from LEO Satellites and Propagated Through Ionospheric Plasma Irregularities

5a. CONTRACT NUMBER
FA9453-19-1-0001

5b. GRANT NUMBER

5c. PROGRAM ELEMENT NUMBER
C6601F

6. AUTHOR(S)
Jiawei Xu, Y. Jade Morton, Dongyang Xu[1], Yu Jiao[2], and Joanna Hinks[3]

5d. PROJECT NUMBER
8466

5e. TASK NUMBER
EF133152

5f. WORK UNIT NUMBER
V1FP

7. PERFORMING ORGANIZATION NAME(S) AND ADDRESS(ES)
University of Colorado Boulder
552 UCB
Boulder, CO 80309-0552

[1]NovAtel, Canada
[2]Trimble Navigation, USA

[3]Air Force Research Laboratory
Space Vehicles Directorate
3550 Aberdeen Avenue SE
Kirtland AFB, NM 87117-5776

8. PERFORMING ORGANIZATION REPORT NUMBER

9. SPONSORING / MONITORING AGENCY NAME(S) AND ADDRESS(ES)
Air Force Research Laboratory
Space Vehicles Directorate
3550 Aberdeen Avenue SE
Kirtland AFB, NM 87117-5776

10. SPONSOR/MONITOR'S ACRONYM(S)
AFRL/RVBYS

11. SPONSOR/MONITOR'S REPORT NUMBER(S)
AFRL-RV-PS-TR-2023-0074

12. DISTRIBUTION / AVAILABILITY STATEMENT
Approved for public release; distribution is unlimited (AFRL-2023-2249 dtd 09 May 2023).

13. SUPPLEMENTARY NOTES

14. ABSTRACT
LEO satellite-based navigation has gained much attention recently. Our earlier simulation study indicated that for signals transmitted from LEO satellites, ionospheric scintillation introduces deeper and more frequent fades and much higher phase dynamics compared to signals transmitted from MEO satellites (Morton et al., 2022). However, there has not been a study on the impact of ionospheric scintillation on the performance of ground-based receiver signal tracking. This paper applies simulated ionospheric plasma irregularity effect on GNSS-like L-band signals transmitted from LEO satellites to assess ground-based receiver signal tracking performance. A physics-based, data-consistent ionosphere scintillation simulator presented by Xu et al. (2020) is used to produce a phase screen model designed to generate realistic strong scintillation effects. The input parameters are extracted from real GPS signal received by a ground station in Hong Kong during a strong ionospheric scintillation event. In this paper, we simulate GPS L1 C/A signals transmitted from LEO orbit, traveling through the phase screen, and received by a stationary receiver on the ground. Multiple scenarios have been simulated assuming phase screens generating different levels of scintillation, LEO satellite orbit parameters, and transmission signal parameters such as amplitude and carrier phase. A total of 9 different space-to-time scale factors associated with these satellite and ionosphere phase screen configurations are considered.

15. SUBJECT TERMS
ionospheric scintillation, LEO satellite navigation, ionospheric simulation, receiver performance

16. SECURITY CLASSIFICATION OF:			**17. LIMITATION OF ABSTRACT**	**18. NUMBER OF PAGES**	**19a. NAME OF RESPONSIBLE PERSON**
a. REPORT	**b. ABSTRACT**	**c. THIS PAGE**			Dr. Joanna C. Hinks
Unclassified	Unclassified	Unclassified	Unlimited	19	**19b. TELEPHONE NUMBER** *(include area code),*

This page is intentionally left blank.

ACKNOWLEDGMENTS

This material is based on research sponsored by Air Force Research Laboratory under agreement number FA9453-19-1-0001. The U.S. Government is authorized to reproduce and distribute reprints for Governmental purposes notwithstanding any copyright notation thereon.

DISCLAIMER

TABLE OF CONTENTS

LIST OF FIGURES

Figure **Page**

LIST OF TABLES

Table **Page**

Tracking GNSS-like Signals Transmitted from LEO Satellites and Propagated Through Ionospheric Plasma Irregularities

Jiawei Xu, *University of Colorado Boulder, USA*
Y. Jade Morton, *University of Colorado Boulder, USA*
Dongyang Xu, *NovAtel, Canada*
Yu Jiao, *Trimble Navigation, USA*
Joanna Hinks, *Air Force Research Laboratory, USA*

BIOGRAPHY

Jiawei Xu is a Ph.D. candidate at the Ann and H.J. Smead Aerospace Engineering Sciences Department, University of Colorado, Boulder. He received his bachelor's degree in aerospace engineering in the School of Aeronautics and Astronautics, Shanghai Jiao Tong University, China in the fall of 2022. His research focuses on the ionospheric scintillation effect on LEO signals, multipath detection and mitigation, and multi-band collaborative tracking.

Y. Jade Morton is Helen and Hubert Croft Professor in the Ann and H.J. Smead Aerospace Engineering Sciences Department at University of Colorado Boulder. Her research interests lie at the intersection of satellite navigation technologies and remote sensing of the Earth's space environment, atmosphere, and surface. She served as a President of the ION and is a member of the US Space-based PNT Advisory Board. She received an AGU SPARC award, ION Burka, Thurlow, and Kepler awards, and IEEE PLANS Richard Kershner award. Dr. Morton received her Ph.D. in EE from Penn State. She is a fellow of IEEE, ION, and UK's Royal Institute of Navigation.

Dongyang Xu is a software engineer at NovAtel. He received his Ph.D. from Colorado State University in 2018, a B.S. from China Agricultural University in 2009, an M.S. from Beihang University, China in 2012 all in Electrical Engineering, and a second M.S. in Computational Engineering and Science from Miami University, Ohio in 2014. His research interests include GNSS software receiver tracking algorithm development and performance analysis under ionospheric scintillation.

Yu Jiao is a software engineer at Trimble Navigation. She worked at the Intel Corporation, shortly after receiving her Ph.D. in Electrical Engineering from Colorado State University in 2017. She received a master's degree in Computational Science and Engineering from Miami University in 2013 and bachelor's degree in Electronic and Information Engineering from Beihang University, China in 2011. Her research interests are in GNSS signal processing and ionosphere effects on GNSS.

Joanna Hinks is the Principal Investigator for the Advanced Signals Team of the Satellite Navigation Technology Area, and Principal Investigator for Navigation Technology Satellite - 3. She works for the Space Vehicles Directorate of the U.S. Air Force Research Laboratory located at Kirtland Air Force Base in Albuquerque, NM. She received her B.S. in Mechanical Engineering in 2002 from Cedarville University, and her M.S. in 2009 and Ph.D. in 2012 from Cornell University, both in Mechanical & Aerospace Engineering. Her research interests include estimation and Kalman filtering, control, and signal processing, with applications ranging from navigation and timing to atomic physics.

ABSTRACT

LEO satellite-based navigation has gained much attention recently. Our earlier simulation study indicated that for signals transmitted from LEO satellites, ionospheric scintillation introduces deeper and more frequent fades and much higher phase dynamics compared to signals transmitted from MEO satellites (Morton et al., 2022). However, there has not been a study on the impact of ionospheric scintillation on the performance of ground-based receiver signal tracking. This paper applies simulated ionospheric plasma irregularity effect on GNSS-like L-band signals transmitted from LEO satellites to assess ground-based receiver signal tracking performance. A physics-based, data-consistent ionosphere scintillation simulator presented by Xu et al. (2020) is used to produce a phase screen model designed to generate realistic strong scintillation effects. The input parameters are extracted from real GPS signal received by a ground station in Hong Kong during a strong ionospheric scintillation event. In this paper, we simulate GPS L1 C/A signals transmitted from LEO orbit, traveling through the phase screen, and received by a stationary receiver on the ground. Multiple scenarios have been simulated assuming phase screens generating different levels of scintillation, LEO satellite orbit parameters, and transmission signal parameters such as amplitude and carrier phase. A total of 9 different space-to-time scale factors associated with these satellite and ionosphere phase screen configurations are considered.

A conventional receiver architecture is implemented to track the simulated signals. Signal amplitude, carrier phase, and tracking loop performances are analyzed. Both case studies and statistical analysis are presented. The impact of ionospheric plasma irregularities on the signal and its tracking process are analyzed and compared with the same signal traveling through the same irregularity, but from a GPS satellite in MEO orbit. Results show that the same ionospheric structure leads to lower C/N0, less stable tracking loop, more loss-of-lock cases, and more cycle slips for the same signals transmitted from LEO than from MEO. And the negative impact is especially serious with LEO signals having higher phase dynamics, as expected. The statistical analysis of the tracking results provides a quantitative understanding of the level of degradation associated with LEO signal tracking during scintillation. The findings in this study will provide insights into signal design and receiver signal processing strategies for future LEO satellite-based PNT systems.

I. INTRODUCTION

LEO satellite-based navigation has been gaining popularity (Reid et al., 2020; Kassas et al., 2021a). Some systems are focused on using communication/network signals transmitted from LEO satellites as signals-of-opportunity for navigation applications (Benzerrouk et al., 2019; Kassas et al., 2021b; Khalife et al., 2020; Orabi et al., 2021). Others utilize dedicated LEO-based navigation signals for GNSS augmentation (Ge et al., 2022; Li et al., 2019; Reid et al., 2018; Yi et al., 2021). All these signals must travel through the ionosphere before reaching receivers on the ground. The ionosphere introduces group delay in range measurements and advance in the carrier phase under quiet conditions, which can be corrected using dual frequency measurements. The more challenging aspect of the ionosphere effect is caused by plasma irregularities which lead to signal amplitude and carrier phase fluctuations, collectively referred to as ionospheric scintillation. The ionospheric scintillation effects on GNSS signals have been well studied (Morton et al., 2020). For signals transmitted from LEO satellites, our earlier study showed that ionospheric scintillation introduces deeper and more frequent fades and much higher phase dynamics compared to signals transmitted from MEO satellites (Morton et al., 2022). However, there has not been a study on the impact of ionospheric scintillation on the performance of ground-based receiver signal tracking.

This paper utilizes simulated ionospheric plasma irregularity effect on GNSS-like L-band signals transmitted from LEO satellites to assess ground-based receiver signal tracking performance. First, a physics-based, data-consistent ionosphere scintillation simulator presented in Jiao et al. (2018); Xu et al. (2020); Rino et al. (2018) is used to produce a phase screen model that is capable of generating strong scintillation. The model generates an abstract statistical representation of the ionospheric irregularities based on real GPS scintillation data collected by a ground-based receiver. We then simulate GPS L1 C/A signals transmitted from several different LEO orbits and traveled through the same phase screen. Code and carrier tracking algorithms are implemented to process the simulated received scintillation signal.

A brief summary of the scintillation simulator and simulation scenarios are presented in Section II. Section III describes the scintillation signal generation and receiver tracking algorithms used in this study. A comparative assessment of the receiver tracking results, including C/N_0 distributions, cycle slips, and loss of lock for the LEO and MEO transmitted signals are provided in Section IV. Section V summarizes the finding.

II. SCINTILLATION SIMULATOR AND SIMULATION SCENARIOS

Figure 1 illustrates the simplified scintillation signal generation and tracking process (detailed diagram and description are given in Section III). Input parameters δ_A, δ_ϕ are scintillation-induced amplitude and carrier phase fluctuation generated by the scintillation simulator (flow chart shown in Figure 2, model parameters defined in Morton et al. (2022)) based on the published model presented in Xu et al. (2020). The simulator establishes the phase screen model based on ground-observed scintillation indicators extracted from real GNSS scintillation signals, and propagation geometry defined by receiver platform dynamics. A plane wave is then propagated through this phase screen realization to obtain the scintillation signal wave fields at the receiver, i.e., δ_A, δ_ϕ. These fluctuation time series are modulated onto the GPS L1 C/A signals, which are simulated to be transmitted from satellites on GPS/custom-defined LEO orbits. Note that the phase screen realization can be placed at desired altitudes h_{PS}, resulting in different fluctuation time series. Therefore, together with LEO altitudes h_{TX}, we are able to simulate scenarios with different phase dynamics.

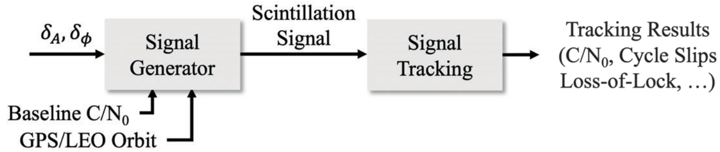

Figure 1: Diagram of scintillation signal generation and tracking process

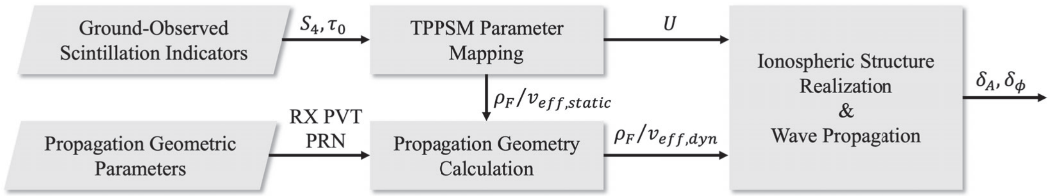

Figure 2: Flow chart of the ionosphere scintillation simulator presented in Xu et al. (2020)

The baseline simulation scenarios (Scenario 1∼4) are the combination of those two sets of parameters: Phase screen altitude at $h_{PS} = 300/500$ km and LEO satellite altitude at $h_{TX} = 550/800$ km. Scenario 0 is a reproduction of the real GPS scintillation signal used in the scintillation simulator in Figure 2. The scheme is illustrated in Figure 3 and was described in detail in Morton et al. (2022). To describe and compare the phase dynamics in each scenario, we compute the decorrelation time τ_0 and list it in Table 1. It indicates how fast the signal fluctuates and smaller values mean higher phase dynamics. We selected 9 representative τ_0 values. For each value, we generate a 500-second scintillation signal carrier phase and amplitude fluctuation time series. The highest and lowest τ_0 values are marked in red and the corresponding sub-scenario are highlighted (highest/lowest is for $0 \sim 300$s instead of 500s to align with the LEO max and min scenarios in Morton et al. (2022)). Since LEO satellites move across much of the sky, the change in both elevation angle and phase dynamics is more significant than the GPS satellite. The variation of elevation and decorrelation time is presented in Figure 4. Places where the τ_0 of each sub-scenario are selected are tagged in each scenario.

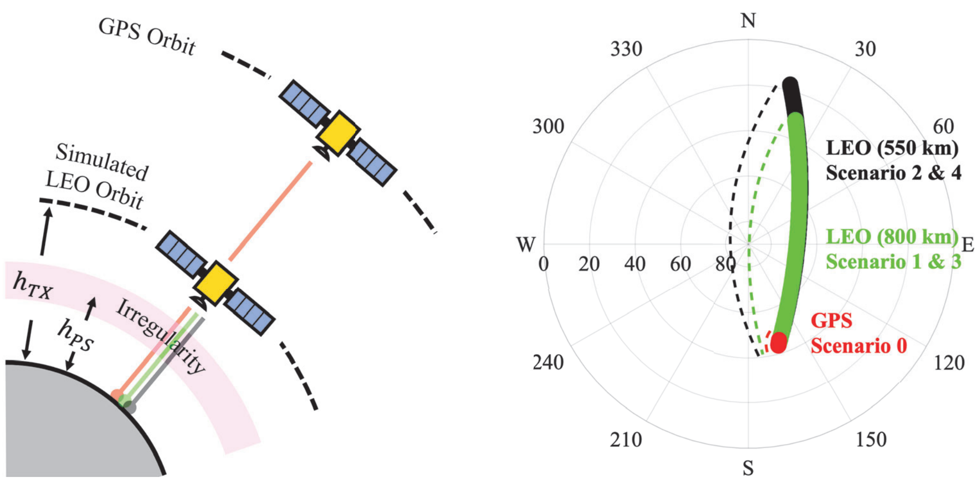

Figure 3: (a) Scintillation simulation configuration. (b) Sky plot of GPS satellite and LEO satellites at 550 and 800km altitude during the 500-second interval

III. SIGNAL GENERATION AND RECEIVER TRACKING ALGORITHM

Figure 5 presents the scintillation signal generation and tracking process in detail. The simulator first generates correlation values directly based on scintillation-induced amplitude and carrier phase fluctuation time series δ_A, δ_ϕ, GPS/LEO satellite orbits, baseline C/N_0 (30 $\sim$ 70 dB-Hz), and coherent integration time T. This method (shown on the right side of Figure 5) follows the same principle as IF signal simulation but has a much lower computation and storage burden (which makes large-scale repeating simulations possible).

The rest of the tracking process basically follows a conventional GNSS receiver architecture. The code and carrier tracking loops are realized by a 2^{nd}-order delay lock loop (DLL) and a $2^{nd}/3^{rd}$-order phase lock loop (PLL) (for GPS/LEO scenario), respectively. The carrier tracking is initialized by a $1^{st}/2^{nd}$-order frequency lock loop (FLL) (for GPS/LEO scenario). In each lock loop, correlation values are fed into a discriminator, which determines the current tracking error and refines local estimates. Both code and carrier tracking are implemented with a Kalman filter (KF) for noise suppression.

For the analysis of tracking results, we first calculate lock detectors (results in Subsection IV.1), which indicates the status of each tracking loop, and estimate C/N_0 (Subsection IV.2) based on correlation values. Cycle slips (Subsection IV.3) and loss-of-lock occurrences (Subsection IV.4) are then detected using the carrier phase estimate, lock detectors, and C/N_0 estimate.

Table 1: Simulation scenarios

Scenario	h_{PS} (km)	h_{TX} (km)	ρ_F/v_{eff} range (s)	τ_0 range (s)	Sub-scenario	Elevation (deg)	τ_0
0	350	MEO	[1.17, 1.19]	[0.79, 0.81]	0.b	44	0.8
1	300	800	[0.24, 0.47]	[0.16, 0.32]	1.a	44	0.16
					1.b	70	0.19
					1.c	31	0.32
2	300	550	[0.16, 0.43]	[0.11, 0.3]	2.a	44	0.12
					2.b	70	0.14
					2.c	18	0.3
3	500	800	[0.2, 0.3]	[0.14, 0.21]	3.b	70	0.14
					3.c	31	0.21
4	500	550	[0.07, 0.14]	[0.05, 0.1]	4.b	70	0.05

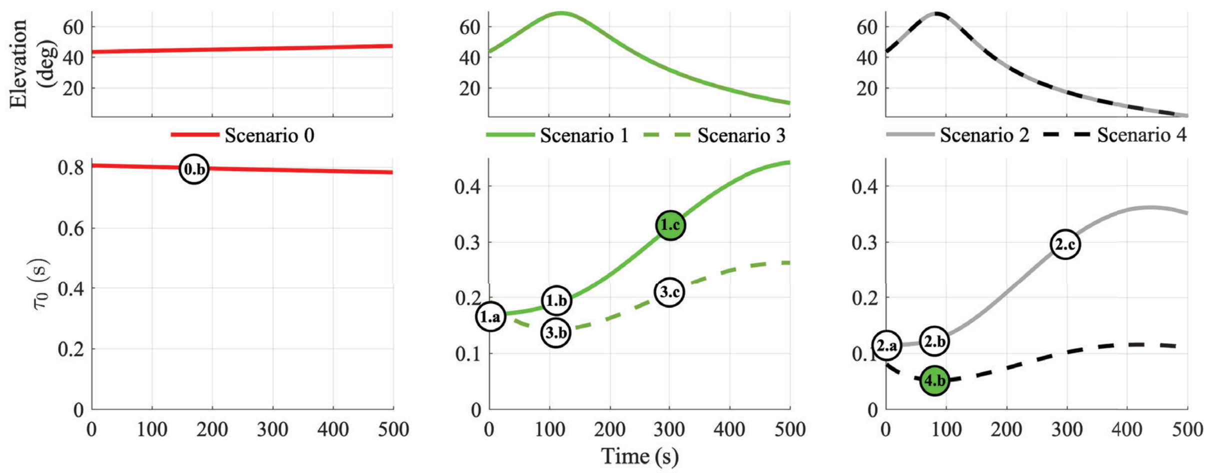

Figure 4: Satellite elevation (top), and decorrelation time τ_0 (bottom) of 5 scenarios duration the 500-second interval

The simulation for each scintillation scenario is repeated 120 times for statistical analysis, and different correlation noise values are generated for each simulation run.

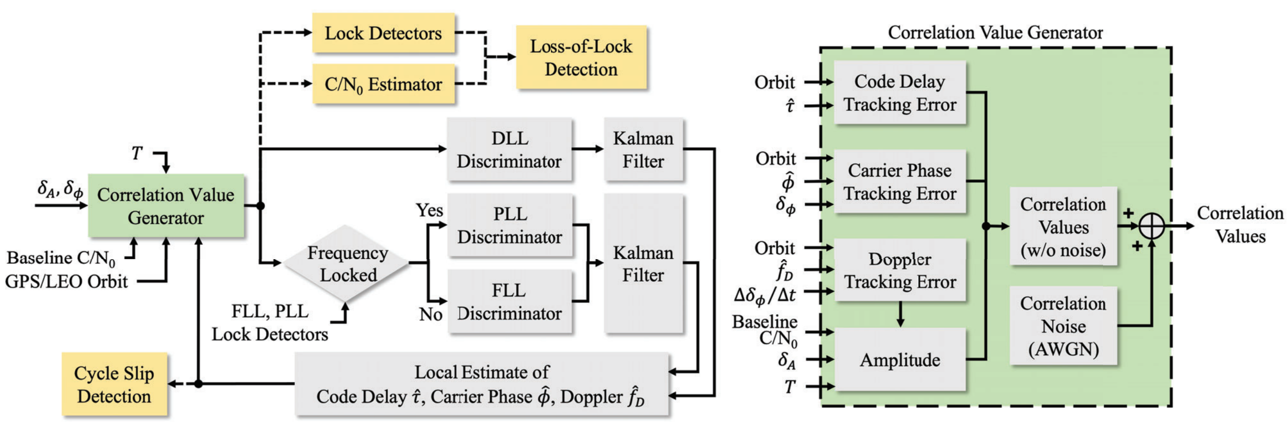

Figure 5: Detailed diagram of scintillation signal generation and tracking process

IV. RESULTS AND ANALYSIS

1. Scintillation Signal Tracking Lock Indicator

Three lock detectors are implemented to indicate the tracking condition of DLL, PLL, and FLL based on correlation values (Mongrédien et al., 2006). The use of the PLL or FLL is dependent on the carrier frequency tracking status as indicated by the FLL lock detector. Measurements from the three lock detectors are averaged over the 500-second interval and the 120 repeating simulations to obtain each loop's state for each scenario and under different C/N_0 conditions. The results are presented in Figure 6. Note that a higher detector value indicates a healthier tracking state. All three subplots show that the tracking loops (especially the PLL and FLL) are in a less healthy state under weaker signal conditions ($\sim$ 30 dB-Hz). The tracking quality improves as C/N_0 increases from 30 to 40 dB-Hz. The best performance comes from signals transmitted by a GPS satellite in MEO (0.b). The worst case is associated with LEO signals having maximum signal dynamics (4.b).

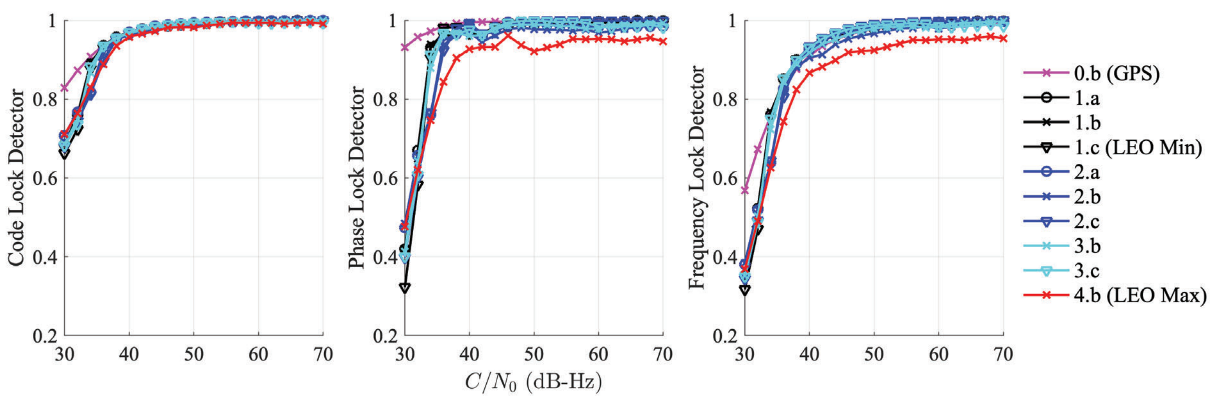

Figure 6: Average DLL, PLL, and FLL lock detector values for each simulation scenario and C/N_0 values

2. C/N_0 Distribution

C/N_0 is an indicator of receiver tracking performance. For each simulation scenario, the signal transmitted from the LEO satellite is set to reach the receiver with a baseline C/N_0 value at 30$\sim$70 dB-Hz. The C/N_0 is estimated by the receiver at a 1-second interval using the variance summing method (VSM) (Sharawi et al., 2007). The estimated C/N_0 deviates from the baseline C/N_0 due to amplitude scintillation, loss-of-lock, tracking error, and C/N_0 estimate error.

The distributions of the estimated C/N_0 for each scenario as a function of its corresponding baseline C/N0 are presented in Figure 7. For all scenarios, there are bimodal distributions at 30 dB-Hz and unimodal for C/N_0 at 40$\sim$70 dB-Hz, indicating that loss-of-lock is prevalent at 30 dB-Hz. The statistical analysis of loss-of-lock at different C/N_0 conditions will be given in subsection IV.4. The shift of distribution peaks towards the left in the LEO scenarios shows that LEO signal tracking is less robust compared to GPS signal when the signal is weak.

3. Cycle Slips

Cycle slip detection is performed on the carrier tracking results, and the cycle slip probability at different times and C/N_0 is calculated from repeat simulations. The time series of carrier phase tracking error in sub-scenario 0.b (GPS), 1.c (LEO min), and 4.b (LEO max) at C/N_0 of 36 and 54 dB-Hz is first presented in Figure 8, where cycle slip is highlighted. Results show that higher phase dynamics and lower C/N_0 lead to more frequent cycle slips. While shorter coherent integration time can theoretically reduce the scintillation effect on carrier tracking loops, it causes more frequent and large cycle slips due to tracking loop instability. Statistical cycle slip results in all 9 scenarios are attached in the Appendix.

We counted the total number of cycle slips in all simulation scenarios. The probability of cycle slip occurrence is shown in Figure 9. Figure 9 (a) and (c) present the probability of cycle slip at different C/N_0 and phase rate disturbance $\Delta\phi/\Delta t$, respectively, while Figure 9 (b) is a heat map that captures the cycle slip dependence on both parameters. Figure 9 (a) shows that cycle slip is more frequent as C/N_0 decreases and peak occurrence is at $\sim$32 dB-Hz. Below 32 dB-Hz, cycle slip becomes less frequent when loss-of-lock dominates (explained in the next subsection) and the PLL becomes unstable (see Figure 6). Figure 9 (b) shows the number of cycle slips increases as the phase rate disturbance strengthens.

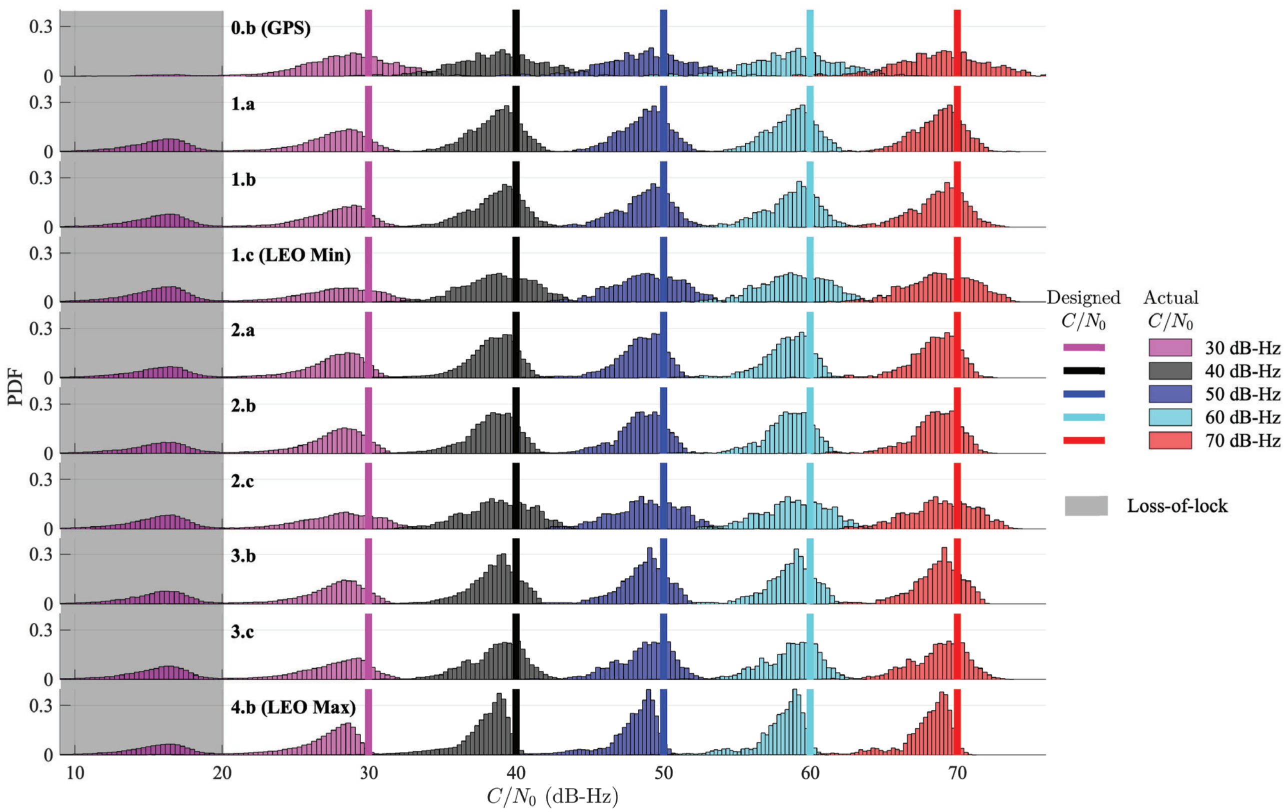

Figure 7: Distributions of receiver estimated C/N_0 dependence on set C/N_0

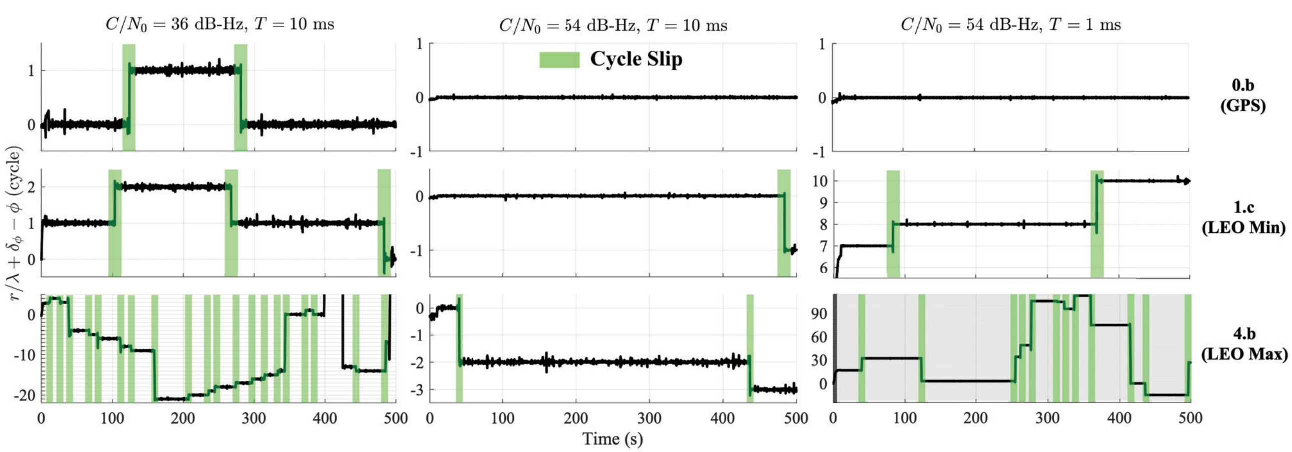

Figure 8: Carrier phase tracking error in sub-scenario 0.b (GPS), 1.c (LEO min), and 4.b (LEO max) at C/N_0 of 36 and 54 dB-Hz

4. Loss-of-lock

The average number of loss-of-lock during the 500-second interval is calculated for all scenarios. The results are displayed in Figure 10. Clearly, the GPS satellite signal (0.b) is much less likely to lose lock than the LEO satellite transmitted signals (1.a $\sim$ 4.b). Among the LEO scenarios, the loss-of-lock probability decreases rapidly as C/N_0 increases from 30 to 40 dB-Hz, and approaches zero once C/N_0 is greater than 40 dB-Hz. Between 35 and 40 dB-Hz, the scenarios (such as 4.b) with higher phase dynamics have a higher loss-of-lock probability.

We also count the total number of loss-of-lock from all 9 LEO scenarios and present the results in Figure 11. Figure 11 (a) and (c) present the probability of loss-of-lock at different C/N_0 and phase rate disturbance $\Delta\phi/\Delta t$, respectively, while Figure 11 (b)

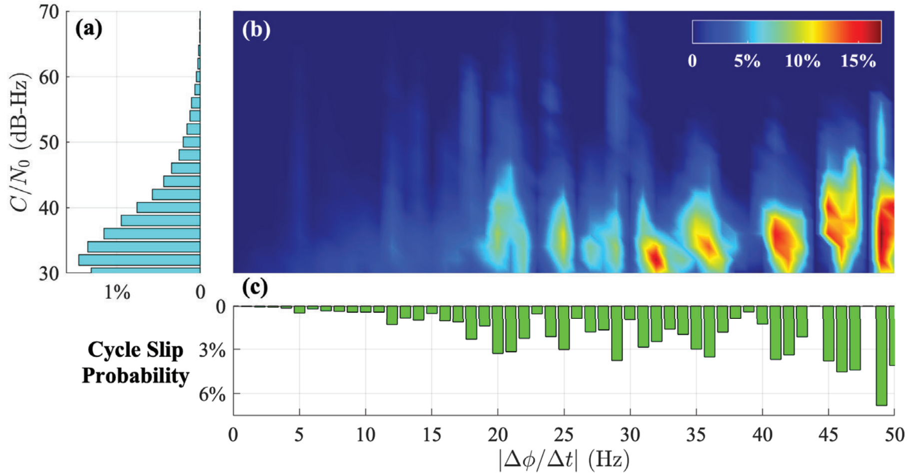

Figure 9: Cycle slip probability at different phase rate disturbance and C/N_0 values

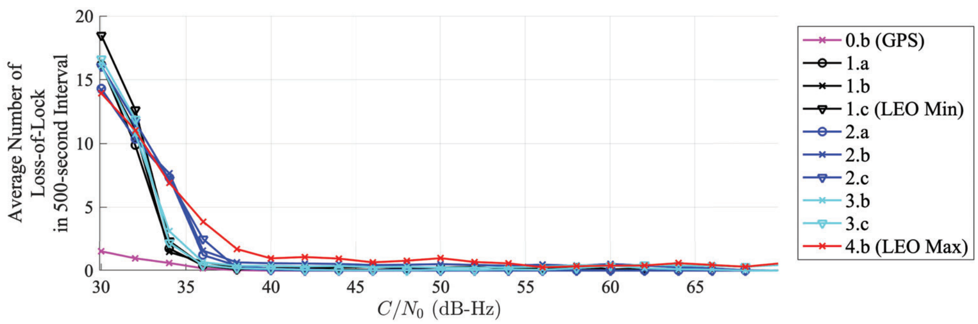

Figure 10: Average number of loss-of-lock during the 500-s interval as function of C/N_0 for each simulation scenario

is the heat map that combines the loss-of-lock dependence on both C/N_0 and phase rate disturbance. Note that the loss-of-lock probability in (c) is calculated from $C/N_0 < 40$ dB-Hz since loss-of-lock seldom occurred for $C/N_0 > 40$ dB-Hz. Figure 11 (c) does not show a strong correlation between the loss-of-lock probability and phase rate disturbance.

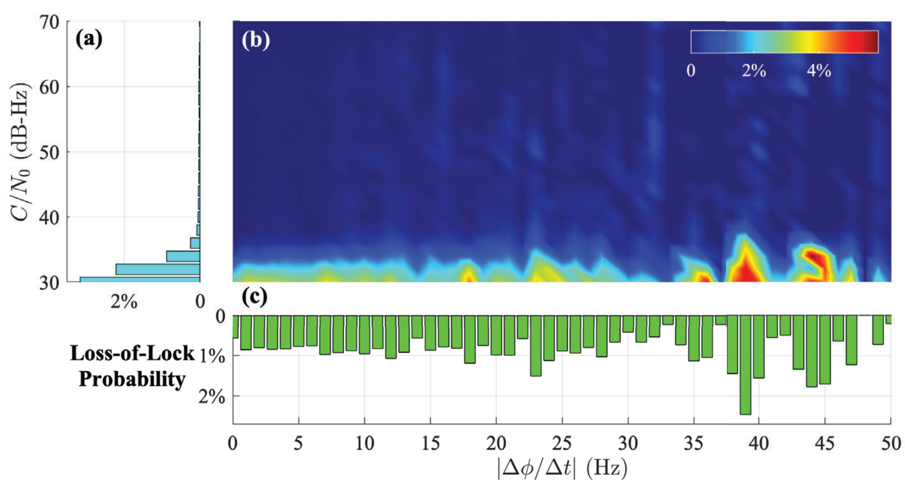

Figure 11: Loss-of-lock probability at different phase rate disturbance and C/N_0

V. CONCLUSIONS

This paper is based on the study of ionospheric scintillation effects on the signal transmitted from LEO satellites by Morton et al. (2022) and focuses on the receiver tracking process of such signals. Multiple scenarios are simulated where the GPS L1 signal propagates from an LEO satellite, traverses a phase screen, and reaches a ground receiver. Two LEO satellite orbits and two phase screen altitudes are simulated for strong but not severe scintillation scenarios defined by a real GNSS scintillation signal. A total of 9 different phase dynamics associated with these satellite and ionosphere phase screen configurations are considered. A conventional DLL/PLL/FLL receiver architecture is implemented to track the simulated signals. The impact of ionospheric plasma irregularities on the signal and its tracking process are analyzed statistically and compared with the same signal traveling through the same irregularity, but from a GPS satellite in the MEO orbit. Results show that scintillation effect on the received signal includes amplitude degradation (as shown in Figure 7) and phase disturbance (Figure 8), which impact receiver tracking algorithms in slightly different ways. Cycle slips are strongly correlated with both C/N_0 and phase rate disturbance (Figure 9), whereas Loss of lock is strongly correlated with C/N_0 but exhibits little or no dependence on phase rate disturbance (Figure 11).

ACKNOWLEDGEMENTS

This work is supported by an AFRL grant (#FA9453-19-1-0001).

REFERENCES

Benzerrouk, H., Nguyen, Q., Xiaoxing, F., Amrhar, A., Nebylov, A. V., and Landry, R. (2019). Alternative PNT based on iridium next LEO satellites Doppler/INS integrated navigation system. In *2019 26th Saint Petersburg International Conference on Integrated Navigation Systems (ICINS)*, pages 1–10. IEEE.

Ge, H., Li, B., Jia, S., Nie, L., Wu, T., Yang, Z., Shang, J., Zheng, Y., and Ge, M. (2022). LEO enhanced global navigation satellite system (LeGNSS): progress, opportunities, and challenges. *Geo-spatial Information Science*, 25(1):1–13.

Jiao, Y., Rino, C., and Morton, Y. T. (2018). Ionospheric scintillation simulation on equatorial GPS signals for dynamic platforms. *Navigation: Journal of The Institute of Navigation*, 65(2):263–274.

Kassas, Z., Morton, J., van Diggelen, F., Spilker, J., and Parkinson, B. (2021a). Navigation from low earth orbit—part 2: Models implementation and performance. In *Position, Navigation, and Timing Technologies in the 21st Century*, volume 2, pages 1381–1412. Wiley.

Kassas, Z., Neinavaie, M., Khalife, J., Khairallah, N., Kozhaya, S., Haidar-Ahmad, J., and Shadram, Z. (2021b). Enter LEO on the GNSS stage: Navigation with starlink satellites.

Khalife, J., Neinavaie, M., and Kassas, Z. M. (2020). Navigation with differential carrier phase measurements from mega-constellation LEO satellites. In *2020 IEEE/ION Position, Location and Navigation Symposium (PLANS)*, pages 1393–1404. IEEE.

Li, B., Ge, H., Ge, M., Nie, L., Shen, Y., and Schuh, H. (2019). LEO enhanced global navigation satellite system (LeGNSS) for real-time precise positioning services. *Advances in space research*, 63(1):73–93.

Morton, Y., Xu, D., and Jiao, Y. (2022). Ionospheric scintillation effects on signals transmitted from LEO satellites. In *Proceedings of the 35th International Technical Meeting of the Satellite Division of The Institute of Navigation (ION GNSS+ 2022)*, pages 2980–2988.

Morton, Y. J., Yang, Z., Breitsch, B., Bourne, H., and Rino, C. (2020). Ionospheric effects, monitoring, and mitigation techniques. *Position, Navigation, and Timing Technologies in the 21st Century: Integrated Satellite Navigation, Sensor Systems, and Civil Applications*, 1:879–937.

Orabi, M., Khalife, J., and Kassas, Z. M. (2021). Opportunistic navigation with Doppler measurements from iridium next and orbcomm LEO satellites. In *2021 IEEE Aerospace Conference (50100)*, pages 1–9. IEEE.

Reid, T. G., Neish, A. M., Walter, T., and Enge, P. K. (2018). Broadband LEO constellations for navigation. *Navigation: Journal of The Institute of Navigation*, 65(2):205–220.

Reid, T. G., Walter, T., Enge, P. K., Lawrence, D., Cobb, H. S., Gutt, G., O'Connor, M., and Whelan, D. (2020). Navigation from low earth orbit: part 1: concept, current capability, and future promise. *Position, Navigation, and Timing Technologies in the 21st Century: Integrated Satellite Navigation, Sensor Systems, and Civil Applications*, 2:1359–1379.

Rino, C., Breitsch, B., Morton, Y., Jiao, Y., Xu, D., and Carrano, C. (2018). A compact multi-frequency GNSS scintillation model. *Navigation*, 65(4):563–569.

Sharawi, M. S., Akos, D. M., and Aloi, D. N. (2007). GPS C/N_0 estimation in the presence of interference and limited quantization levels. *IEEE transactions on aerospace and electronic systems*, 43(1):227–238.

Xu, D., Morton, Y. J., Rino, C. L., Carrano, C. S., and Jiao, Y. (2020). A two-parameter multifrequency GPS signal simulator for strong equatorial ionospheric scintillation: modeling and parameter characterization. *NAVIGATION: Journal of the Institute of Navigation*, 67(1):181–195.

Yi, H., Lei, W., Wenju, F., Haitao, Z., Tao, L., Beizhen, X., and Ruizhi, C. (2021). LEO navigation augmentation constellation design with the multi-objective optimization approaches. *Chinese Journal of Aeronautics*, 34(4):265–278.

A. CYCLE SLIP PROBABILITY IN ALL SCENARIOS

The cycle slip probability in all 9 scenarios is shown in Figure 12 using heat maps, together with corresponding phase rate disturbance. In the bottom plot, all epochs with over 40% probability of cycle slip are highlighted to reveal their correlation with phase rate disturbance. In each highlighted area, an impulse of phase rate disturbance can be spotted, which indicates that the cycle slip is likely triggered by extreme phase rate disturbance.

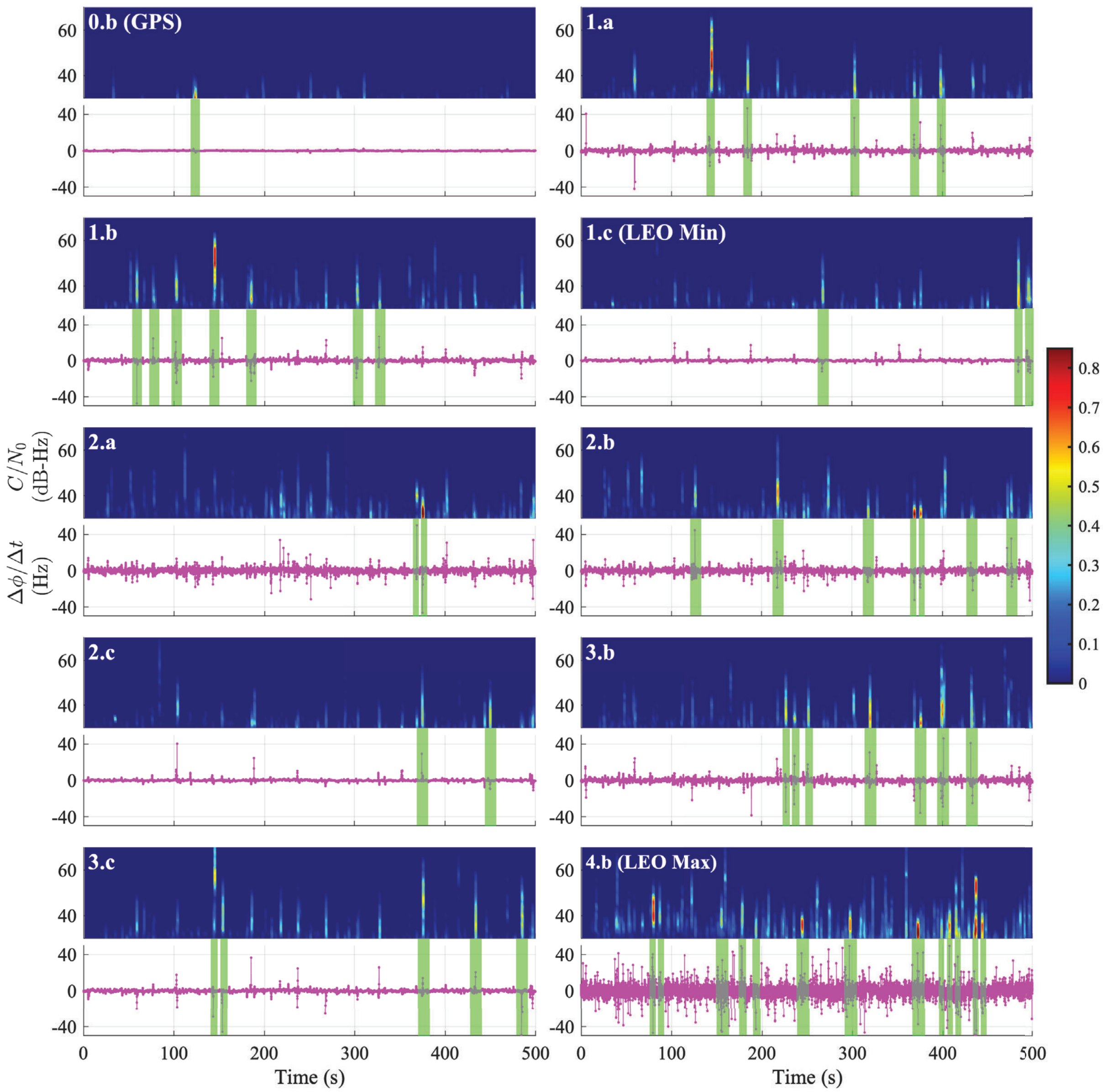

Figure 12: Cycle slip probability at different times and C/N_0 (top) calculated from repeat simulations and corresponding phase rate disturbance (bottom)

DISTRIBUTION LIST

DTIC/OCP 8725 John J. Kingman Rd, Suite 0944 Ft Belvoir, VA 22060-6218	1 cy
AFRL/RVIL Kirtland AFB, NM 87117-5776	1 cy
Official Record Copy AFRL/RVB/Dr. Joanna C. Hinks	1 cy

This page is intentionally left blank.